

The Modeling of Synfuel Production Process

ASPEN Model of FT production with electricity demand provided at LWR scale

December | 2021

Guiyan Zang, Pingping Sun, Amgad Elgowainy

Systems Assessment Center, Energy Systems Division, Argonne National Laboratory



IES

Integrated Energy Systems

DISCLAIMER

This information was prepared as an account of work sponsored by an agency of the U.S. Government. Neither the U.S. Government nor any agency thereof, nor any of their employees, makes any warranty, expressed or implied, or assumes any legal liability or responsibility for the accuracy, completeness, or usefulness, of any information, apparatus, product, or process disclosed, or represents that its use would not infringe privately owned rights. References herein to any specific commercial product, process, or service by trade name, trade mark, manufacturer, or otherwise, does not necessarily constitute or imply its endorsement, recommendation, or favoring by the U.S. Government or any agency thereof. The views and opinions of authors expressed herein do not necessarily state or reflect those of the U.S. Government or any agency thereof.

The Modeling of Synfuel Production Process

ASPEN Model of FT production with electricity demand provided at LWR scale

Guiyan Zang, Pingping Sun, Amgad Elgowainy
Systems Assessment Center, Energy Systems Division, Argonne National
Laboratory

December 30, 2021

Argonne National Laboratory
Lemont, Illinois 60439

Prepared for the
U.S. Department of Energy
Office of Nuclear Energy
Under DOE Argonne Site Office
Contract DE-AC02-06CH11357

Page intentionally left blank

ABSTRACT

Synfuels, or electro-fuels (e-fuels) have the unique potential to significantly reduce greenhouse gas (GHG) emissions across the transportation sector. This is especially true for applications with substantial payloads and daily miles traveled, such as long-haul heavy-duty vehicles, rail locomotives, marine vessels and aviation aircrafts that are challenging to directly electrify via battery or fuel cell powertrain technologies. Synfuels, or electro-diesel/electro-jet fuels, have similar properties with the incumbent petroleum fuels, compatible with current infrastructure but have much lower GHG emissions relative to the petroleum counterpart, because they utilize waste carbon dioxide (CO₂) streams and green hydrogen (H₂) sourced from electrolysis. To achieve substantial reductions in GHG emissions, electricity sources must be zero carbon or near-zero carbon, which is the case with solar, wind, hydro and nuclear power. Compared to the intermittency of solar, wind and hydro, nuclear energy provides a steady energy source. In addition, it's advantageous for nuclear power to produce synfuels because it provides not only near-zero carbon electricity to displace grid electricity, but also near-zero carbon steam to displace carbon-intensive natural gas combustion for steam generation. The availability of electricity and steam also enables more efficient green hydrogen production by using high-temperature electrolysis. In this work, Argonne National Laboratory (ANL) models a synfuel production process via the Fischer- Tropsch (FT) reaction by using nuclear power to provide electricity and steam. In 2021, using ASPEN Plus software, ANL established a detailed process model of a stand-alone FT production facility, assuming feedstocks of pure CO₂ and H₂. This stand-alone model can be expanded to integrate H₂ production from nuclear power via low-temperature and high-temperature electrolysis at light-water reactor (LWR) scale.

This report summarizes the stand-alone ASPEN Plus model results with a detailed mass and energy analysis. Our modeled facility produces 351 MT/day (130,000 gal/day) of FT fuel (a mixture of naphtha, jet fuel, and diesel) by converting 223 MT/day of H₂ and 2,387 MT/day of CO₂. The FT fuel production energy efficiency is 58% and the carbon conversion efficiency (from CO₂ to FT fuel) is 46%. The production of green hydrogen requires 390–470 MWe of electricity, which is compared with the capacity of an LWR plant.

For the stand-alone FT process, the detailed energy demand (electricity and heat) is summarized in the table below.

Based on the energy supply source and the required temperature, potential insertion points of nuclear energy are identified. Based on the potential nuclear energy utilization, this report discusses potential modification options for expanding the system boundary to integrate nuclear power use, for example on-site hydrogen production via water electrolysis. Modeling of the integrated system is conducted by closely

working with ANL and Idaho National Laboratory (INL) collaborators to harmonize design parameters of nuclear plants and the FT production process.

Table Abstract-1. Energy consumption and production in the stand-alone FT fuel production process

Area	Electricity (GJ/hr)	Electricity source	Heat (GJ/hr)	Heat source	Steam (GJ/hr)	Steam source
A1 H ₂ and CO ₂ compression	-42.8	Nuclear electricity and power generated on-site				
A2 RWGS reaction	-25.0	Power generated on-site	-105.6	Direct heating from tail gas combustion		
A3 FT-synthesis	-0.9	Power generated on-site	238.7 (<220 °C)	FT reactors and gas cooling		
A4 hydro-processing			-54.1	Heat exchange		
A5 power generation	+58.9	Power generated on-site	+105.6	Direct heating from tail gas combustion	+54.1	Heat exchange
A6 utility	-3.1	Power generated on-site	-247.3 (<220 °C)	Cooling tower		
Nuclear electricity	+12.9					

Note: Green indicates that the energy source can be replaced by a nuclear source; red color indicates that the energy might be supplied by direct heating for high temperature.

Page intentionally left blank

CONTENTS

1.	INTRODUCTION.....	6
1.1	FT fuels synthesis	6
1.2	Nuclear reactor scale for FT fuel synthesis.....	7
2.	ASPEN MODEL OF FT SYNTHESIS AT LWR SCALE	8
2.1	System design.....	8
2.2	A1 H₂ and CO₂ compression and A2 RWGS reaction	11
2.3	A3 FT-synthesis	12
2.4	A4 Hydro-processing	14
2.5	A5 Power generation and A6 Utility.....	16
3.	MASS AND ENERGY CONVERSION RESULTS.....	17
4.	POTENTIAL PROCESS MODIFICATION USING NUCLEAR ENERGY	19
5.	CONCLUSIONS	21
6.	REFERENCES	21

FIGURES

Figure 1-1. Major processes and reactions in synthetic FT fuel production	7
Figure 1-2. Nuclear reactor scale and H₂ production capacities ^[7]	8
Figure 2-1. System flowchart for liquid fuel production from H₂ and CO₂ based on the FT process.....	9
Figure 2-2. A2 RWGS reaction area flowchart for syngas produced from CO₂ and H₂	12
Figure 2-3. A3 FT-synthesis area flowchart for hydrocarbon produced from syngas	13
Figure 2-4. Distribution of hydrocarbons produced from the FT synthesis reactor with carbon numbers from 1 to 20	13
Figure 2-5. A4 hydro-processing area flowchart for FT fuel production	15
Figure 2-6. Distribution of hydrocarbons produced from the hydro-processing reactor with carbon numbers from 1 to 20	15
Figure 2-7. A5 Power generation area flowchart for power and heat supplement	16
Figure 3-1. Mass Sankey diagram for FT fuel production.....	18
Figure 4-1. Boundary expansion potential.....	20

TABLES

Table 2-1. FT fuel synthesis, plant scale and electricity demand from an LWR plant.....	9
Table 2-2. ASPEN Plus simulation results for major flow shown in Figure 2-1	10
Table 2-3. Heat needed for the RWGS reaction.....	12
Table 2-4. Heat released from FT synthesis	14
Table 2-5. CHP system design parameters	17
Table 3-1. Energy inputs/outputs and efficiencies of the ASPEN Plus model	17
Table 3-2. Mass inputs/outputs and carbon conversion efficiency of the ASPEN Plus model.....	18
Table 4-1. Energy consumption and production in the stand-alone FT fuel production process.....	19

The Modeling of Synfuel Production Process

ASPEN Model of FT production with electricity demand provided at LWR scale

1. INTRODUCTION

Synthetic fuels (synfuels) or electro-fuels (e-fuels) are drop-in hydrocarbon fuels that source energy from electricity. Synfuels have the unique potential to significantly reduce greenhouse gas (GHG) emissions across the transportation sector. This is especially true for applications with substantial payloads and daily miles traveled, such as long-haul heavy-duty vehicles, rail locomotives, marine vessels and aviation aircrafts that are challenging to directly electrify via battery or fuel cell powertrain technologies.[1] To achieve substantial reductions in GHG emissions, electricity sources must be zero carbon or near-zero carbon, which is the case with solar, wind, hydro and nuclear power.[2]

As with other low-carbon fuel technologies, the reduction of carbon emissions is usually achieved at a premium over the price of existing conventional fuels. Earlier modeling and analysis by Argonne National Laboratory (ANL) showed that hydrogen cost dominates synfuel production cost.[3] Thus, to reduce synfuel cost to approach conventional petroleum fuel costs, the cost of hydrogen needs to be near \$1/kg.[3] Nuclear and perhaps hydro-power are low-carbon sources that have the potential to produce hydrogen for less than \$2/kg, much lower than the cost of hydrogen produced by intermittent wind or solar power. This is due to three main factors: (1) the sustained supply of nuclear power improves utilization of the electrolyzer, and thus spreads its capital cost over a larger amount of hydrogen production during its lifetime; (2) the sustained supply of nuclear power avoids the need for significant hydrogen storage, which is required to mitigate intermittency issues with wind and solar power, thus further reducing the cost of hydrogen for synfuel production; and (3) nuclear power has the potential to be paired with high-temperature electrolysis (HTE; e.g., SOEC technology, using Solid oxide electrolyzer cell), which has considerably increased hydrogen production efficiency compared to low-temperature electrolysis (LTE; e.g., PEM technology, using polymer electrolyte membranes), thus further reducing the production cost of near-zero carbon hydrogen.[4]

1.1 FT fuels synthesis

Among the commonly researched synfuels, Fischer-Tropsch (FT) fuels (jet, diesel, as well as a lesser amount of naphtha) are particularly attractive for transportation applications because of their applications in heavy-duty vehicles and aviation, compatibility with conventional petroleum fuels for blending and compatibility with the existing infrastructure.[3]

FT fuels are produced via the FT reaction from syngas, which is, in turn, produced from converting carbon dioxide (CO₂) and hydrogen (H₂), as shown in Figure 1-1. H₂ can be sourced from water electrolysis with near-zero carbon electricity (e.g., nuclear), while carbon dioxide can be sourced from various waste streams with various purities. For example, CO₂ waste streams from ethanol plants and ammonia plants are in near-pure form, thus CO₂ capture from these streams has both a low energy penalty and a low cost. The feedstock H₂ and CO₂ are converted into syngas (i.e., the mixture of carbon monoxide (CO) and H₂) by a reverse water gas shift (RWGS) reaction.[5] The resultant syngas is then converted to hydrocarbons with carbon chains ranging from C1-C30, via the FT reaction.[6] Through distillation, liquid hydrocarbons (C4-C20 for naphtha, jet fuel and diesel) are separated and collected as final product. The heavier portion (C20-C30) is further processed with additional hydrogen via a hydrocracking reaction, and the resultant products are distilled into different carbon chain lengths to blend with existing gasoline, jet and diesel fuels.[3]

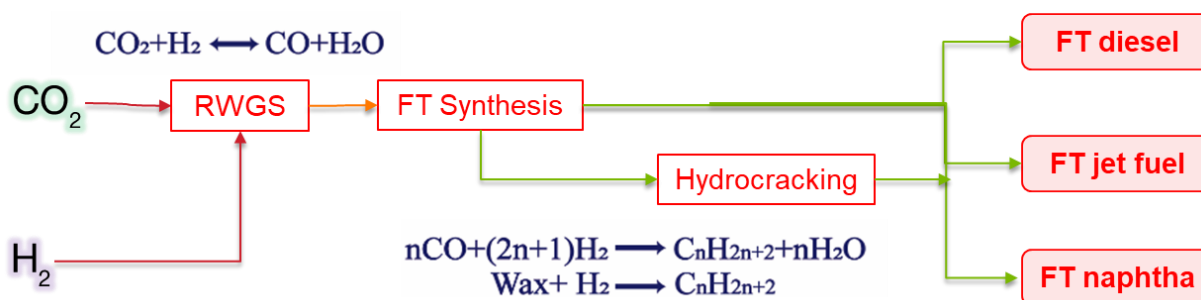


Figure 1-1. Major processes and reactions in synthetic FT fuel production

1.2 Nuclear reactor scale for FT fuel synthesis

Nuclear power is one of the largest and most reliable domestic sources of clean energy in the U.S., which produced 55% of emission-free electricity in 2018. [7] Figure 1-2 shows three nuclear reactor scale groups (large, small, and micro) with concepts under development. The current commercial nuclear reactors in the U.S., which are in the large-scale group (300–1,000+ MWe), were built in the 1950s–1980s and are difficult to scale due to their high investment cost.[7] Some small-scale reactors (20–300 MWe), called small modular reactors (SMR), are under development. The first SMR is currently going through the regulatory approval process and is expected to operate by 2029.[8] Small-scale nuclear reactors can produce electricity, heat, and steam for large utilities, municipalities and industrial applications. SMRs are designed to be modular; thus, the reactor scale can be increased readily by adding SMR modules as demand increases. [7] The third group is microreactors (1–20 MWe), which have the potential to supply power, heat, and steam for remote locations, maritime shipping, military installations, space missions and industrial applications. Similar to the SMR reactors, the scale of microreactors can be modified easily by adding and removing modules. [7]

Nuclear reactors can provide green hydrogen for FT fuels production with near-zero carbon emissions. HTE is a technology for producing hydrogen from water at high temperature with an energy efficiency of approximately 80%. [4] Low-temperature electrolysis (LTE) is another water electrolysis technology for hydrogen production that has an energy efficiency around 66%. [9] Figure 1-2 shows the H₂ production capacities of using electricity from nuclear plants of various scales through HTE and LTE technologies. For a large-scale light water reactor (LWR) plant that has a capacity of 300–1,000 MWe, the H₂ production capacities of HTE and LTE technologies are 170–580 metric ton/day (MT/day) and 140–480 MT/day, respectively.




Nuclear reactor scale	Large (300~1,000+MWe)	Small (20~300MWe)	Micro (1~20MWe)
			
H ₂ production from HTE (efficiency 80%)	170~580 metric ton/day	12~170 metric ton/day	0.6~12 metric ton/day
H ₂ production from LTE (efficiency 66%)	140~480 metric ton/day	10~140 metric ton/day	0.5~10 metric ton/day

Figure 1-2. Nuclear reactor scale and H₂ production capacities [10–12]

This report describes the model development process for a stand-alone FT production facility using the ASPEN Plus model, which can be expanded to integrate nuclear powered electrolysis. For the given FT plant scale, hydrogen demand is comparable with the production capacity of an LWR nuclear power plant. This report introduces the detailed process design, mass and energy balance. Furthermore, this report discusses potential modifications to the initial model to expand the system boundary to include power generation and heat supply from a nuclear power plant.

2. ASPEN MODEL OF FT SYNTHESIS AT LWR SCALE

2.1 System design

By considering the economics of scales for FT fuels production, we modeled a FT fuel synthesis facility that produces 130,000 gal/day of FT fuel using 223 MT/day of H₂ (Table 2-1). This amount of hydrogen requires 390 MWe of electricity using HTE or 470 MWe of electricity using LTE technology (Table 2-1). This scale is within the range of a large LWR plant, which usually has the capacity to produce 140–480 MT H₂/day, as shown in Figure 1-2. The detailed process is shown in Figure 2-1.

Table 2-1. FT fuel synthesis, plant scale and electricity demand from an LWR plant

Electricity demand (HTE) for H ₂	Electricity demand (LTE) for H ₂	H ₂ demand	FT fuel production
390 MWe	470 MWe	223 MT/day	130,000 gal/day

As shown in Figure 2-1, the FT fuel production pathway consists of six process areas, namely, A1 H₂ and CO₂ compression, A2 RWGS reaction, A3 FT-synthesis, A4 hydro-processing, A5 power generation and A6 utility. The ASPEN Plus simulation results for major flow paths are listed in Table 2-2.

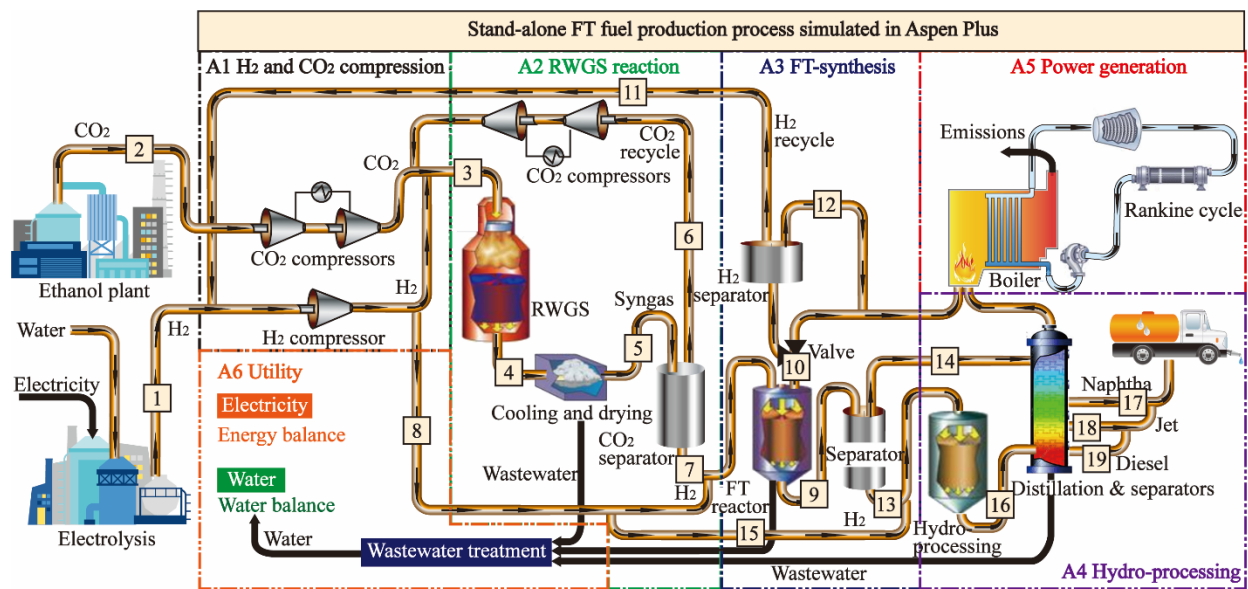


Figure 2-1. System flowchart for liquid fuel production from H₂ and CO₂ based on the FT process

For the stand-alone FT production system, the simulation boundary starts from a pure H₂ source (flow 1 of 223 MT/day) and a pure CO₂ source (flow 2 of 2,387 MT/day) to produce a FT fuel mixture of naphtha (flow 17 of 90 MT/day), jet fuel (flow 18 of 164 MT/day), and diesel (flow 19 of 97 MT/day). The sources of H₂ and CO₂ will be considered when the system boundary is expanded to include the upstream of H₂ production and CO₂ supply.

In compression area (A1), the H₂ and CO₂ feedstocks are compressed to 25 bar. In the A2 RWGS reaction area, H₂ reacts with CO₂ (with a CO₂/H₂ molar ratio equal to 1.0) through the RWGS reaction (R1) at 600 °C and 24.5 bar to produce syngas flow 4,[13] with one pass conversion of 36%. The resultant gas mixture is cooled and dried to remove water. The remaining gas mixture, syngas flow 5, passes through a Selexol CO₂ separator to recover and recycle the unconverted CO₂ (flow 6) and produce flow 7 of syngas.[14] Flow 7 has a H₂/CO molar ratio of 1.8, which is used as the feedstock for the A3 FT synthesis area.[6]

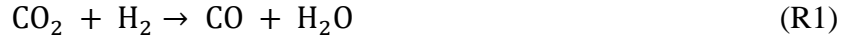
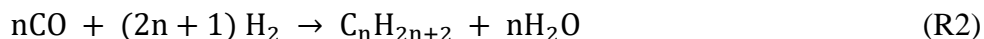


Table 2-2. ASPEN Plus simulation results for major flow shown in Figure 2-1

Flow number	1	2	3	4	5	6	7	8	9	10
Temperature (°C)	25.0	25.0	67.9	600.0	43.0	50.1	220.0	49.8	210.0	43.0
Pressure (bar)	20.0	1.0	24.7	24.5	22.7	3.4	30.0	24.7	24.0	22.7
Mass flowrate (MT/day)	223	2,387	5,317	5,317	833	2,701	1,880	31	702	833
Mole flowrate (kmol/hr)	4,599	2,260	9,599	9,599	1,873	2,611	5,343	642	810	1,873
Mole fraction (%)										
H ₂ O	0.0	0.0	0.0	17.7	0.3	0.0	0.0	0.0	91.0	0.3
CO	0.0	0.0	1.5	19.2	20.5	5.6	31.8	0.0	0.0	20.5
H ₂	100.0	0.0	49.3	31.5	52.2	0.0	57.8	100.0	0.0	52.2
CO ₂	0.0	100.0	49.2	31.5	25.0	94.4	10.4	0.0	0.0	25.0
CH ₄	0.0	0.0	0.0	0.0	0.2	0.0	0.0	0.0	0.0	0.2
C ₂ H ₆	0.0	0.0	0.0	0.0	0.6	0.0	0.0	0.0	0.0	0.6
C _n H _{2n+2}	0.0	0.0	0.0	0.0	0.8	0.0	0.0	0.0	7.0	0.8
Wax	0.0	0.0	0.0	0.0	0.0	0.0	0.0	0.0	2.0	0.0
Other	0.0	0.0	0.0	0.0	0.4	0.0	0.0	0.0	0.0	0.4
Flow number	11	12	13	14	15	16	17	18	19	
Temperature (°C)	43.0	27.8	210.0	150.0	49.8	233.1	30.0	30.0	30.0	
Pressure (bar)	22.7	1.2	24.0	23.0	24.7	23.0	1.0	1.0	1.0	
Mass flowrate (MT/day)	40	792	205	182	3	407	90	164	97	
Mole flowrate (kmol/hr)	831	1,042	24	56	60	142	33	40	17	
Mole fraction (%)										
H ₂ O	0.0	0.6	0.3	13.1	0.0	5.2	0.1	0.0	0.0	
CO	0.0	36.9	0.1	0.0	0.0	0.0	0.0	0.0	0.0	
H ₂	100.0	14.1	0.0	0.0	100.0	17.6	0.0	0.0	0.0	
CO ₂	0.0	44.9	1.4	0.0	0.0	0.2	0.0	0.0	0.0	
CH ₄	0.0	0.4	0.2	0.4	0.0	0.8	0.0	0.0	0.0	
C ₂ H ₆	0.0	1.0	0.1	0.0	0.0	0.0	0.0	0.0	0.0	
C _n H _{2n+2}	0.0	1.4	33.2	86.2	0.0	74.8	99.9	100.0	100.0	
Wax	0.0	0.0	64.7	0.3	0.0	1.2	0.0	0.0	0.0	
Other	0.0	0.8	0.0	0.0	0.0	0.0	0.0	0.0	0.0	

In the A3 FT-synthesis area, the syngas (flow 7) from A2 reacts with high-pressure H₂ (flow 8 from A1) to form liquid hydrocarbons (flow 9) and light gas (flow 10) through a reaction (R2) with various chain lengths.[6] The resultant stream (flow 10) mainly consists of CO, H₂ and C1–C5 hydrocarbons that flow through a H₂ pressure swing adsorption (PSA) separator to recover and

recycle the unconverted H₂ (flow 11).[15] The PSA tail gases, which are combustible gases (flow 12), are utilized in the A5 power generation area. The liquid hydrocarbons (flow 9 with major components of C₅–C₃₀) are produced from the bottom of the FT synthesis reactor. A separator is used to separate flow 9 into the heavier cut (C₂₀–C₃₀, called wax, flow 13) for hydrocracking and the lighter cut (C₅–C₂₀, flow 14) for distillation.[16]



In the A4 hydro-processing area, the wax (flow 13) from A3 reacts with high-pressure H₂ (flow 15 from A1) to be cracked into lighter hydrocarbons <C₂₀, which are further separated into naphtha, jet fuel and diesel. The naphtha (flow 17) has a boiling point lower than 141 °C, jet fuel (flow 18) has a boiling point of 141–207 °C, and diesel (flow 19) has a boiling point of 207–290 °C.[17] The A5 power generation and A6 utility areas are auxiliary reaction areas. All the combustible light gases from other reaction areas are fed into a boiler in the A5 power generation area to generate power and supply heat for the system via a Rankine cycle. Meanwhile, the A6 utility area consists of wastewater treatment, a cooling tower, a water supply, and products storage.[2] More detailed technical information about the ASPEN Plus model is supplied in the following sections.

2.2 A1 H₂ and CO₂ compression and A2 RWGS reaction

The first reaction area, A1 H₂ and CO₂ compression, evaluates the power demand for H₂ and CO₂ compression. The initial pressures of CO₂ and H₂ are assumed to be 1 bar and 20 bar, respectively.[18,19] Because the RWGS reactor is operated at 24.5 bar, H₂ and CO₂ are compressed to 25 bar in the A1 H₂ and CO₂ compression area. Three compressors are used in A1 H₂ and CO₂ compression, with an isentropic efficiency of 86%: (a) a five-stages CO₂ input compressor with an intercooler's temperature of 43 °C; (b) a three-stages CO₂ recycle compressor with an intercooler's temperature of 43 °C; and (c) a one-stage H₂ compressor without intercoolers.

The second area, A2 RWGS reaction, contains the RWGS reaction, syngas cooling and drying, compressors (not shown in the simple flowchart but simulated in the ASPEN Plus model) and the CO₂ separator, as shown in Figure 2-2. The RWGS reaction modeled in the current research is based on the experimental result of Kim *et al.* using BaCe_{0.2}Zr_{0.6}Y_{0.16}Zn_{0.04}O₃ as the catalyst.[20] The RWGS reaction takes place at 600 °C and 24.5 bar with a CO₂ conversion ratio of 36% with an H₂/CO₂ input molar ratio of 1.0.[20] The RWGS reaction is an endothermic reaction at 600 °C, with the heat supplied by direct combustion of light gases from the total system, as listed in Table 2-3. In addition, the feedstock of CO₂/H₂ needs to be preheated from 486 °C to 600 °C, requiring 44.5 GJ/hr heat (flow 3 in Figure 2-1), which is supplied via direct combustion.

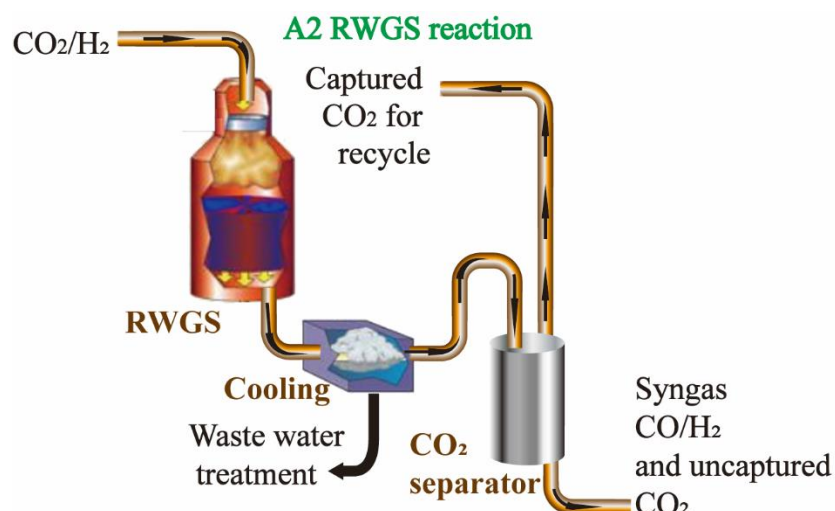


Figure 2-2. A2 RWGS reaction area flowchart for syngas produced from CO₂ and H₂

Table 2-3. Heat needed for the RWGS reaction

RWGS reaction, 600 °C			
RWGS reaction heat needed	17.0 MWt	61.1	GJ/hr
CO₂/H₂ preheating heat needed	12.4 MWt	44.5	GJ/hr

Syngas produced from the RWGS reaction is cooled to 43 °C and then dried and compressed to 30 bar using a five-stages intercooling compressor. The Selexol CO₂ separation unit uses ethylene glycol as a solvent that absorbs CO₂ in the absorber at 30 bar and releases CO₂ from flash tanks at 3.4 bar, 1.0 bar and 0.3 bar for CO₂ recycling.[14] The total compression power consumption of the A2 RWGS reaction area is 25 GJ/hr. The syngas produced from the Selexol CO₂ separation unit is used as feedstock for the FT synthesis reaction in the A3 FT-synthesis area.

Meanwhile, the water produced from the RWGS reaction is separated from the produced syngas by flasher and separator after cooling to 43 °C and is subsequently treated by the wastewater treatment process in the A6 utility area.

2.3 A3 FT-synthesis

The A3 FT-synthesis area consists of two FT fixed-bed reactors, wax/liquid/gas separators, and one PSA H₂ separator. A simplified flow chart is shown in Figure 2-3. The FT reactors feed an H₂/CO mixture with a molar ratio of 2.2 and use cobalt-based catalysts to convert 52.2% of CO (from syngas flow from the A2 RWGS reaction area) into hydrocarbons at 220 °C and 24.3 bar.

The hydrocarbon product distribution is defined using the Anderson-Schulz-Flory distribution shown in Equation (1):[21]

$$\log(W_n/n) = n \times \log \alpha + \log [(1 - \alpha)^2 / \alpha] \quad (1)$$

where α is 0.9, n is the carbon number in C_nH_{2n+2} produced from the FT reaction (R3) and W_n is the mass ratio of C_nH_{2n+2} in the total hydrocarbon production distribution. The distribution of C_nH_{2n+2} with carbon numbers from 1 to 20 is shown in Figure 2-4. Both the mass ratio and molar ratio of hydrocarbons with carbon numbers from 1 to 20 are illustrated in Figure 2-4, whereas the heavier hydrocarbons are assumed to have an average carbon number of 30.[17]

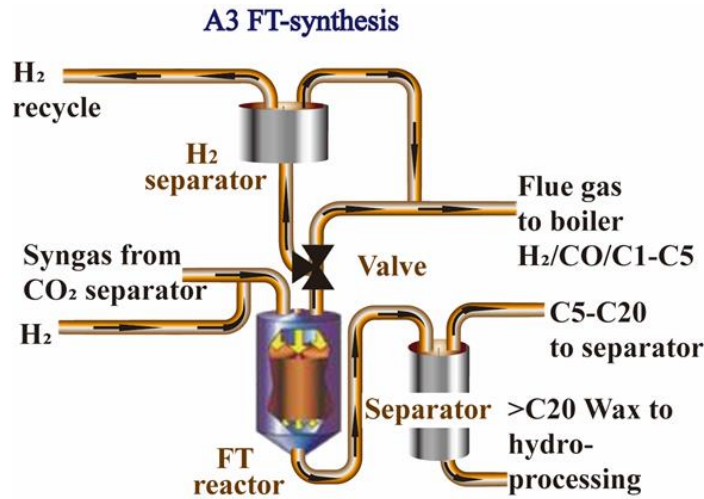
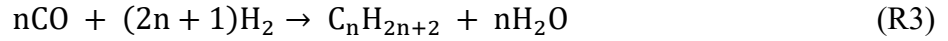


Figure 2-3. A3 FT-synthesis area flowchart for hydrocarbon produced from syngas

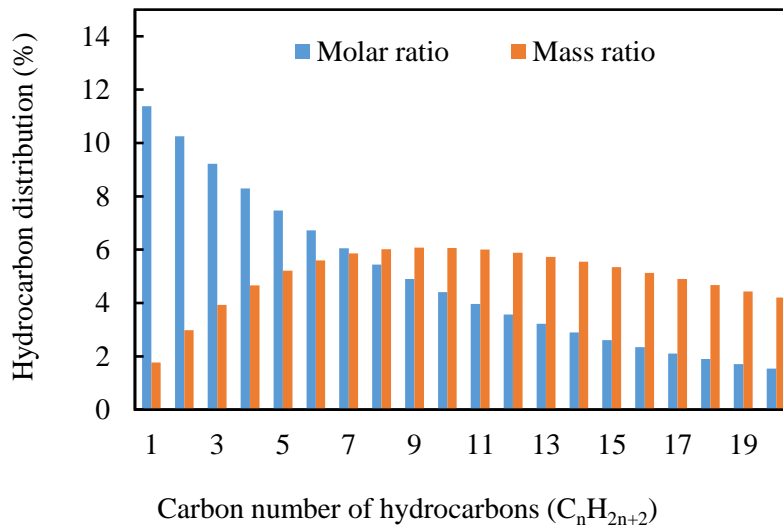


Figure 2-4. Distribution of hydrocarbons produced from the FT synthesis reactor with carbon numbers from 1 to 20

The FT synthesis reaction is exothermic. The reactor is cooled by a cooling tower to maintain an operating temperature of 220 °C. The first FT synthesis reactor released -142.5 GJ/hr heat and the second FT synthesis reactor released -59.4 GJ/hr with a constant temperature of 220 °C, as shown in Table 2-4. The heat released from the FT synthesis reaction is due to changes in the chemical composition of the FT synthesis reaction, which has a constant temperature of 220 °C. When the produced flue gas is cooled from 220 °C to 43 °C, -23.0 GJ/hr and -13.8 GJ/hr heat is released. Heat released from the FT synthesis reaction and gas cooling processes can be used to generate low-pressure steam (5 bar, 151°C) to capture CO₂ from stationary sources using methyl diethanolamine (MDEA) technology,[22] if the boundary is expanded to include the CO₂ capture processes.

Table 2-4. Heat released from FT synthesis

Flow number	GJ/hr	Inlet °C	Outlet °C	Note
Q-R-FL	-142.5	220	220	Heat released from FT reactor 1
QRGAS	-23.0	220	43	Heat released for gas cooling 1
Q-R-FL-2	-59.4	220	220	Heat released from FT reactor 2
QRGAS-2	-13.8	220	43	Heat released for gas cooling 2

Flue gases with the major components H₂/CO/C1–C5 are produced from the top of the FT reactor. A PSA unit is used to separate and recycle unconverted H₂ (85% efficiency) in the flue gas with a high purity of 99.9% at 23.2 bar.[15] Tail gases from the PSA unit are combusted in the A5 power generation area to supply power and heat for the total system. Hydrocarbons produced from the bottom of the FT reactor are flashed to separate heavier hydrocarbons (wax >C₂₀) from lighter hydrocarbons (C₅–C₂₀) at 220 °C. The wax is cooled (to condense the water) and dried for hydrocracking, while the lighter hydrocarbons are distilled to produce liquid fuels in the A4 hydro-processing area. The total syngas compression power consumption of A3 FT synthesis is 1 GJ/hr.

2.4 A4 Hydro-processing

The fourth processing area, A4 Hydro-processing, mainly includes a hydro-processing reactor and a fuel distillation tower, as shown in Figure 2-5. The hydro-processing process cracks 89% of the wax into lighter hydrocarbons at 290 °C and 23.2 bar. The distribution of hydrocarbon produced (shown in Figure 2-6) is defined based on the work of Kang *et al.*[16], which conducted tests over the Pt/Si–Al catalyst. Both the molar ratio and mass ratio of hydrocarbons with carbon numbers from 1 to 20 are illustrated in Figure 2-6. The unconverted wax is recycled to the hydro-processing reactor. The FT fuel (including naphtha, jet fuel and diesel) is produced from the A4 Hydro-processing area. The lighter hydrocarbons (C₅–C₂₀) from hydro-processing and the A3 FT synthesis area are separated into liquid products of naphtha (90 MT/day), which has a boiling point

below 141 °C, jet fuel (164 MT/day), which has a boiling point of 141–207 °C, and diesel (97 MT/day), which has a boiling point of 207–290 °C, by distillation.[17]

The hydro-processing reaction and light hydrocarbon distillation process take place at an elevated temperature (<290 °C) and need an energy input of 54.1 GJ/hr. In the current ASPEN Plus model, 54.1 GJ/hr heat is provided by steam generated from the turbine in the A5 power generation area, given the temperature is less than 290 °C. After the system boundary is expanded to include the LWR plant, steam/heat from the secondary side of the nuclear plant can be used in lieu of heat provided by steam from the local combined heat and power generation steam.

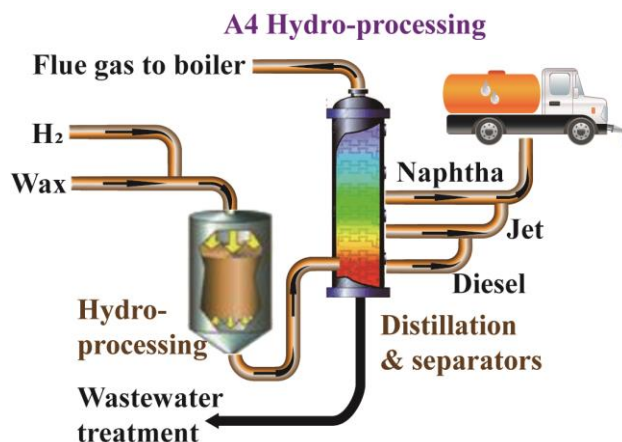


Figure 2-5. A4 hydro-processing area flowchart for FT fuel production

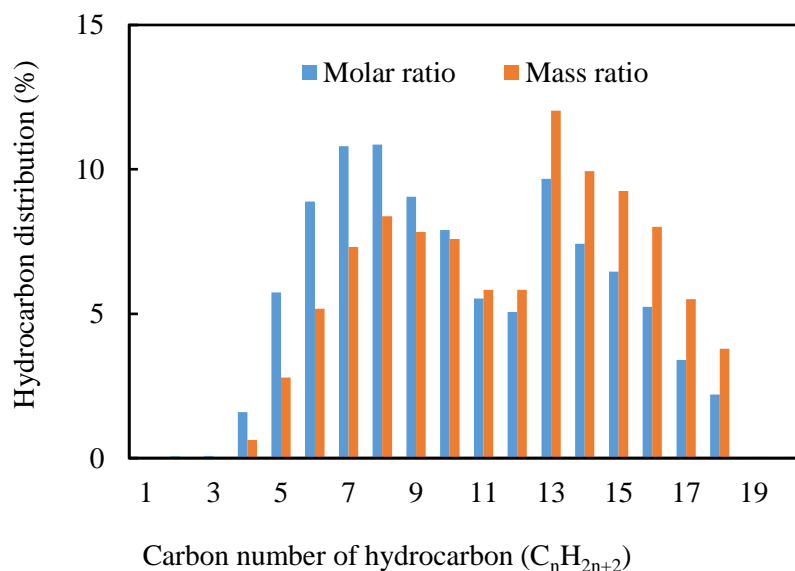


Figure 2-6. Distribution of hydrocarbons produced from the hydro-processing reactor with carbon numbers from 1 to 20

2.5 A5 Power generation and A6 Utility

All the combustible light gases (tail gases) from the other reaction areas are combusted to generate power via a steam turbine and supply heat via direct combustion and steam, as shown in Figure 2-7.[23] The steam turbine uses steam at 505 °C and 103 bar and has an isentropic efficiency of 88%. Table 2-5 shows the direct combustion and combined heat and power (CHP) system design parameters. In the RWGS reaction area, 105.6 GJ/hr direct heat is supplied via direct combustion for the RWGS reaction and H₂/CO₂ preheating. In the A4 hydro-processing area, 54.1 GJ/hr steam heat is used for the hydro-processing and distillation processes. In the A5 power generation area, 58.9 GJ/hr of power is generated from the steam turbine to drive compressors used in the total system. Table 2-5 also shows the energy efficiency of the direct combustion and CHP system design based on the lower heating value (LHV). The power generation efficiency of the direct combustion and CHP plant is 17.7%, according to the total LHV of the tail gases. The heat efficiency of the direct combustion heat supplied to the RWGS reaction area is 31.8%. The steam heat efficiency of the steam heat supplied for hydrocracking and distillation is 16.3%. Thus, the total energy efficiency of the direct combustion and CHP plant used in the ASPEN Plus model is 65.8%.

When the stand-alone FT process is integrated to utilize energy from the LWR plant energy, the power generation designed in A5 can be eliminated by using nuclear electricity. Process steam can also potentially be supplied by the LWR plant to avoid boiler use. This will be investigated and reported in a future publication.

The A6 utility area evaluates the water and energy exchange/balance for the total system. This area includes wastewater treatment, cooling towers and product storage units. The wastewater treatment is simulated using a separator in the ASPEN Plus model. The cooling tower is designed to have an initial cooling temperature of 28 °C and a returning water temperature of 37 °C, with a cooling water recycling efficiency of 99.85%.[15] For the total system, all the pumps have the same isentropic efficiency of 78%.[23]

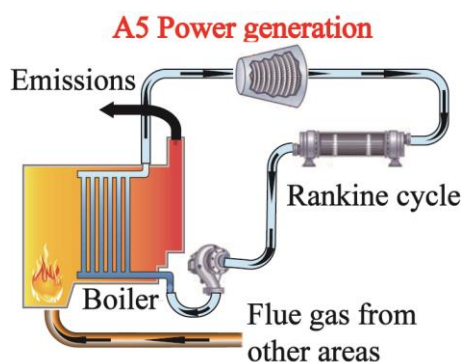


Figure 2-7. A5 Power generation area flowchart for power and heat supplement

Table 2-5. CHP system design parameters

CHP system design	Values	Note
LHV of tail gas, GJ/hr	332.2	Fuel input for A5
Direct heat used, GJ/hr	105.6	Direct combustion heat supply for A2
Steam heat used, GJ/hr	54.1	Steam heat supply from the steam turbine for A4
Power generation, GJ/hr	58.9	Steam turbine power generation
Power efficiency	17.7%	Power generation/LHV of residual gas
Direct heat efficiency	31.8%	Direct heat used/LHV of residual gas
Steam heat efficiency	16.3%	Steam heat used/LHV of residual gas
Total CHP efficiency	65.8%	Total power and heat/ LHV of residual gas

3. MASS AND ENERGY CONVERSION RESULTS

The energy inputs/outputs and efficiencies of the stand-alone FT fuel production process are shown in Table 3-1. The energy inputs are H₂ and electricity, and the system energy outputs are FT liquid fuel (including naphtha, jet fuel and diesel). H₂ is the energy source used in the system, with a LHV of 1,112 GJ/hr. The total power consumption of compressors and pumps in the total system is 72 GJ/hr, but only 59 GJ/hr of power is generated from the A5 Power generation area. Thus, an additional 13 GJ/hr of electricity is needed from an external source (e.g., nuclear power plant). As energy outputs of the system, naphtha, jet fuel and diesel have LHVs of 168 GJ/hr, 302 GJ/hr, and 177 GJ/hr, respectively. Therefore, the total FT fuel production efficiency of the designed system is 58%. It is worth mentioning that the stand-alone system is designed to maximize the on-site energy supply (electricity, heat and steam), enabling the FT facility to be operated in remote areas in the proximity of a H₂ or CO₂ source. Given the potential integration with a nuclear power supply, the system design can be modified to increase energy efficiency by reducing light gas combustion via increasing H₂ and CO₂ recovery.

Table 3-1. Energy inputs/outputs and efficiencies of the ASPEN Plus model

Energy balance	Energy type	
Input energy (GJ/hr)	H ₂ energy	1,112
	Electricity	13
Output energy (GJ/hr)	Naphtha	168
	Jet fuel	302
	Diesel	177
FT fuel production efficiency (%)		58%

In the FT fuels production system designed, 223 MT/day of H₂ and 2,387 MT/day of CO₂ are converted into 351 MT/day of total liquid FT fuels with a product mass ratio of 1/1.82/1.08 (naphtha/jet fuel/diesel), as shown in Table 3-2. The carbon content of the CO₂ source is 651 MT/day, in which 297 MT/day of carbon is converted into liquid FT fuels (naphtha, jet fuel, and diesel), and the other 354 MT/day of carbon is emitted to the atmosphere as combustion emissions to generate electricity, heat and steam. The FT fuel carbon conversion efficiency of the total system design is 46%.

The mass Sankey diagram for the integrated system per GJ of FT fuel is shown in Figure 3-1, where all values are in the unit kg per GJ of FT fuel production. The width of the flow indicates the quantity of mass, green boxes represent conversion processes, and blue, black, and brown flows represent materials flows of H₂, wastewater, and other materials, respectively. The production of 1 GJ of FT fuels or 22.6 kg of FT fuels consumes 153.8 kg of CO₂ and 14.4 kg of H₂.

Table 3-2. Mass inputs/outputs and carbon conversion efficiency of the ASPEN Plus model

Mass balance	Mass type	
Input mass (MT/day)	H ₂	223
	CO ₂	2,387
Output mass (MT/day)	Naphtha	90
	Jet fuel	164
	Diesel	97
FT fuel carbon conversion efficiency (%)	46%	

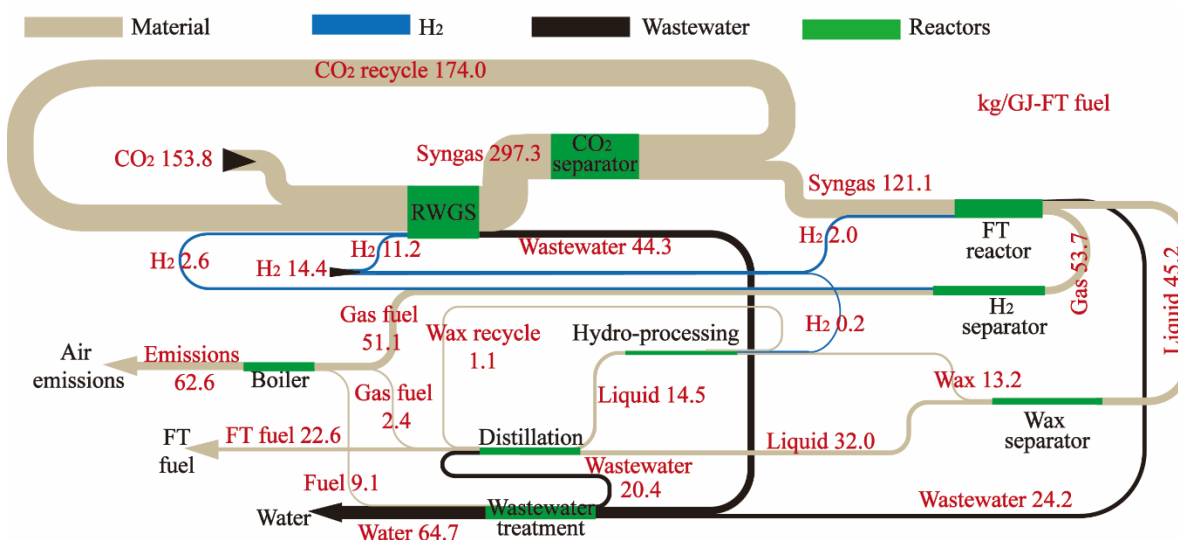


Figure 3-1. Mass Sankey diagram for FT fuel production

4. POTENTIAL PROCESS MODIFICATION USING NUCLEAR ENERGY

Currently, the FT process is designed for a stand-alone facility using feedstocks of pure CO₂ and pure H₂ (assuming they are supplied from pipelines), with the modeled process described above, the facility energy use is summarized in Table 4-1.

Table 4-1. Energy consumption and production in the stand-alone FT fuel production process

Area	Electricity (GJ/hr)	Electricity source	Heat (GJ/hr)	Heat source	Steam (GJ/hr)	Steam source
A1 H ₂ and CO ₂ compression	-42.8	Nuclear electricity and power generated on-site				
A2 RWGS reaction	-25.0	Power generated on-site	-105.6	Direct heating from tail gas combustion		
A3 FT-synthesis	-0.9	Power generated on-site	238.7 (<220 °C)	FT reactors and gas cooling		
A4 hydro-processing			-54.1	Heat exchange		
A5 power generation	+58.9	Power generated on-site	+105.6	Direct heating from tail gas combustion	+54.1	Heat exchange
A6 utility	-3.1	Power generated on-site	-247.3 (<220 °C)	Cooling tower		
Nuclear electricity	+12.9					

Note: Green indicates that the energy source can be replaced by a nuclear source; red indicates that the energy might be supplied by direct heating for high temperature.

Table 4-1 labels potential opportunities to use nuclear energy for FT production, based on electricity and steam demands. Considering the integration of FT production with nuclear energy production, several modification options are considered in the expanded system to increase efficiency and minimize CO₂ emissions and production costs, as shown in Figure 4-1.

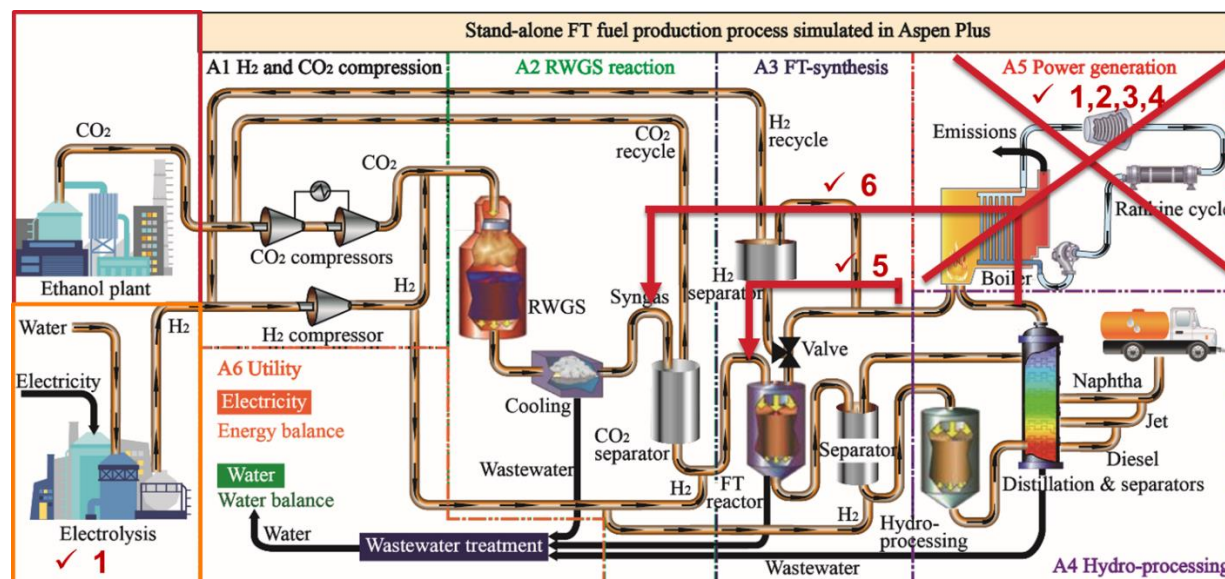


Figure 4-1. Boundary expansion potential

1. Instead of using pure H₂ sources, H₂ gas can be supplied on-site from an electrolysis unit using nuclear power. Thus, the system inputs are CO₂ and electricity (instead of H₂), and potentially steam if heat integration with nuclear power plant is feasible. Given the electrolyzer is on-site, oxygen (O₂) gas is also co-produced on-site. O₂ gas can be sold to generate additional revenue or used for oxy-combustion of light gases (e.g., to heat the RWGS reaction), replacing the current air combustion process. The oxy-combustion process results in high purity CO₂ that can be recycled as feedstock without using the costly carbon capture unit.
2. The system also consumes a large amount of electricity for compressors and pumps. The power demand can be supplied by a nuclear power plant directly.
3. The steam needed for the hydro-processing and distillation processes in the A4 Hydro-processing area can be supplied by steam generated from a nuclear power plant. Given the availability of nuclear electricity and steam, the on-site CHP (for power generation) can be eliminated.
4. Process light gases (C₁–C₄ hydrocarbons, H₂ and CO) are generated from distillation, hydrocracking, and the PSA unit as tail gas. Light gases can be combusted for direct heating

(e.g., for the RWGS reaction), which requires a high temperature (600 °C). If surplus light gases are generated, further reforming of these gases (by converting C1–C4 hydrocarbons to syngas with CO₂) will be investigated.

5. Process light gases have no market outlets, so they need to be utilized on-site. Recycling residual gas from the A3 FT-synthesis area to the FT reactor increases the CO conversion ratio of the FT reactors. This modification reduces the amount of CO in the light gases, and thus has the potential to avoid the production of surplus light gases.
6. After the residual gas is recycled to the FT reactor, unreacted CO₂ accumulates in the light gas from the A4 hydro-processing area. Recycling light gas from the A4 hydro-processing area to the CO₂ separator increases the CO₂ recycle ratio, and thus increases the FT fuel carbon conversion efficiency.

5. CONCLUSIONS

In this work, ANL developed a detailed stand-alone FT production facility in ASPEN Plus with CO₂ and H₂ as inputs. The ASPEN Plus model consists of six process areas: A1 H₂ and CO₂ compression, A2 RWGS reaction, A3 FT-synthesis, A4 hydro-processing, A5 power generation and A6 utility. In the ASPEN Plus model, 223MT/day of H₂ and 2,387 of CO₂ are used to produce 351 MT/day of liquid FT fuels (including naphtha, jet fuel and diesel), with a FT fuel production energy efficiency of 58% and a FT fuel carbon conversion efficiency of 46%. This report introduces the ASPEN Plus model with a detailed mass and energy conversion analysis. For the stand-alone design, most of the facility's energy demand is supplied via on-site energy generation by light gas combustion.

This model can be expanded to include H₂ production from nuclear power via LT and HT electrolysis at the LWR scale. With a H₂ demand of 223 MT/day, the current design can be integrated with a large-scale LWR plant for FT fuel production from CO₂ and nuclear electricity (for H₂ production).

We developed a stand-alone ASPEN Plus model. Based on the detailed energy and mass analysis of each reaction area, this report provides several modification options to utilize electricity and heat from nuclear power plants, while reducing on-site combustion and improving energy efficiency as well as carbon conversion efficiency.

6. REFERENCES

- [1] Zang G, Sun P, Yoo E, Elgowainy A, Bafana A, Lee U, et al. Synthetic Methanol/Fischer–Tropsch Fuel Production Capacity, Cost, and Carbon Intensity Utilizing CO₂ from Industrial and Power

- Plants in the United States. *Environ Sci Technol* 2021. <https://doi.org/10.1021/acs.est.0c08674>.
- [2] Zang G, Sun P, Elgowainy A, Bafana A, Wang M. Life-Cycle Analysis of Electro-fuels: Fischer-Tropsch Fuel Production from Hydrogen and Corn Ethanol By-product CO₂. *Environ Sci Technol* 2021;55:3888–97. <https://doi.org/https://doi.org/10.1021/acs.est.0c05893>.
- [3] Zang G, Sun P, Elgowainy A, Bafana A, Wang M. Performance and cost analysis of liquid fuel production from H₂ and CO₂ based on the Fischer-Tropsch process. *J CO₂ Util* 2021;46. <https://doi.org/https://doi.org/10.1016/j.jcou.2021.101459>.
- [4] S&P Global Platts. Ceres targets solid oxide electrolyzers for hydrogen in industrial processes, e-fuels 2021. <https://www.spglobal.com/platts/en/market-insights/latest-news/electric-power/070121-ceres-targets-solid-oxide-electrolyzers-for-hydrogen-in-industrial-processes-e-fuels>.
- [5] Jurković DL, Pohar A, Dasireddy VDBC, Likozar B. Effect of Copper-based Catalyst Support on Reverse Water-Gas Shift Reaction (RWGS) Activity for CO₂ Reduction. *Chem Eng Technol* 2017;40:973–80. <https://doi.org/10.1002/ceat.201600594>.
- [6] Swanson RM, Platon A, Satrio JA, Brown RC, Hsu DD. Techno-Economic Analysis of Biofuels Production Based on Gasification. United States: 2010. <https://doi.org/10.2172/994017>.
- [7] Office of Nuclear Energy. Nuclear Reactor Technologies 2020. <https://www.energy.gov/ne/nuclear-reactor-technologies>.
- [8] NuScale Power L. NuScale SMR Technology: An Ideal Solution for Repurposing U.S. Coal Plant Infrastructure and Revitalizing Communities. Corvallis, Oregon: 2021.
- [9] James, Brian; Colella, Whitney; Moton, Jennie; Saur, G.; Ramsden T. PEM Electrolysis H₂A Production Case Study Documentation. United States: 2013. <https://doi.org/10.2172/1214980>.
- [10] THIRD WAY. Nuclear Reimagined. <https://www.thirdway.org/blog/nuclear-reimagined>.
- [11] Office of Nuclear Energy. Light Water Reactor Sustainability (LWRS) Program 2020. <https://www.energy.gov/ne/nuclear-reactor-technologies/light-water-reactor-sustainability-lwrs-program>.
- [12] Office of Nuclear Energy. Advanced Small Modular Reactors (SMRs). 2020 n.d. <https://www.energy.gov/ne/advanced-small-modular-reactors-smrs>.
- [13] Anicic B, Trop P, Goricanec D. Comparison between two methods of methanol production from carbon dioxide. *Energy* 2014;77:279–89. <https://doi.org/https://doi.org/10.1016/j.energy.2014.09.069>.
- [14] Doctor RD, Molburg JC, Thimmapuram PR. KRW oxygenblown gasification combined cycle: carbon dioxide recovery, transport and disposal. Argonne National Laboratory/ENS report. ANL/ESD-34, August; 1996.
- [15] Spath P, Aden A, Eggeman T, Ringer M, Wallace B, Jechura J. Biomass to Hydrogen Production Detailed Design and Economics Utilizing the Battelle Columbus Laboratory Indirectly-Heated Gasifier. United States: 2005. <https://doi.org/10.2172/15016221>.
- [16] Kang J, Ma W, Keogh RA, Shafer WD, Jacobs G, Davis BH. Hydrocracking and Hydroisomerization of n-Hexadecane, n-Octacosane and Fischer–Tropsch Wax Over a Pt/SiO₂–Al₂O₃ Catalyst. *Catal Letters* 2012;142:1295–305. <https://doi.org/10.1007/s10562-012-0910-5>.
- [17] Skone Albany, OR (United States)] TJ [National ETL (NETL), Marriott Inc., McLean, VA (United States)] J [Booz AH, Cooney Inc., McLean, VA (United States)] G [Booz AH, Jamieson Inc., McLean, VA (United States)] M [Booz AH, Jones Inc., McLean, VA (United States)] C

- [Booz AH, Hakian Inc., McLean, VA (United States)] J [Booz AH, et al. Comprehensive Analysis of Coal and Biomass Conversion to Jet Fuel: Oxygen Blown, Entrained-Flow Gasifier (EFG) and Fischer-Tropsch (F-T) Catalyst Configurations Modeled and Validated Scenarios. United States: 2015. <https://doi.org/10.2172/1513807>.
- [18] Dutta, Abhijit; Sahir, Asad; Tan, Eric; Humbird, David; Snowden-Swan, Lesley J.; Meyer, Pimphan; Ross, Jeff; Sexton, Danielle; Yap, Raymond; Lukas JL. Process Design and Economics for the Conversion of Lignocellulosic Biomass to Hydrocarbon Fuels. Thermochemical Research Pathways with In Situ and Ex Situ Upgrading of Fast Pyrolysis Vapors. United States: 2015. <https://doi.org/10.2172/1215007>.
- [19] Lee D-Y, Elgowainy A. By-product hydrogen from steam cracking of natural gas liquids (NGLs): Potential for large-scale hydrogen fuel production, life-cycle air emissions reduction, and economic benefit. *Int J Hydrogen Energy* 2018;43:20143–60. <https://doi.org/https://doi.org/10.1016/j.ijhydene.2018.09.039>.
- [20] Kim DH, Park JL, Park EJ, Kim YD, Uhm S. Dopant Effect of Barium Zirconate-Based Perovskite-Type Catalysts for the Intermediate-Temperature Reverse Water Gas Shift Reaction. *ACS Catal* 2014;4:3117–22. <https://doi.org/10.1021/cs500476e>.
- [21] Fazeli H, Panahi M, Rafiee A. Investigating the potential of carbon dioxide utilization in a gas-to-liquids process with iron-based Fischer-Tropsch catalyst. *J Nat Gas Sci Eng* 2018;52:549–58. <https://doi.org/https://doi.org/10.1016/j.jngse.2018.02.005>.
- [22] Herron S, Zoelle A, Summers WM. Cost of Capturing CO₂ from Industrial Sources. NETL; 2014.
- [23] Zang G, Tejasvi S, Ratner A, Lora ES. A comparative study of biomass integrated gasification combined cycle power systems: Performance analysis. *Bioresour Technol* 2018;255:246–56. <https://doi.org/https://doi.org/10.1016/j.biortech.2018.01.093>.